IJE TRANSACTIONS C: Aspects Vol. 32, No. 9, (September 2019) 1248-1259

International Journal of Engineering

Journal Homepage: www.ije.ir

Seismic Yield Displacement Profile in Steel Eccentrically Braced Frames

M. J. Zahedi, H. Saffari*

Department of Civil Engineering, Shahid Bahonar University of Kerman, Kerman, Iran

P A P E R I N F O

Paper history:
Received 09 January 2019
Received in revised form 24 June 2019
Accepted 05 July 2019

Keywords:
Seismic Yeild Displacement
Direct Displacement based Design
Performance Based Seismic Design
Eccentrically Braced Frames
Steel Building

A B S T R A C T

Displacement-based methods are recognized as appropriate approaches to reach the goals of performance-based seismic design method. In the direct displacement-based seismic design method, the seismic yield displacement is applied as one of the important design parameters. In this paper, a new relation is suggested to determine the lateral displacement pattern at first yielding of eccentrically braced frame systems subjected to earthquake ground motions. This relation considers the influence of various structural features of frames. It is developed from the results of several nonlinear dynamic analyses containing 30 eccentrically braced frames under 15 far-field and near-field earthquake ground motions. Then, the results of these analyses are processed by nonlinear regression analysis in order to establish the most effective parameters on the yield displacement pattern of the frames. As a result, a comparison between the suggested yield displacement pattern and nonlinear dynamic analyses showed the efficiency and advantages of the suggested approach.

***doi**: 10.5829/ije.2019.32.09c.04*

1. INTRODUCTION

Performance-based seismic design (PBSD) strives to design structures with specific performance goals. Performance levels are expressed in terms of displacements as damage is better correlated with displacements in comparison with forces [1, 2]. Displacement-based design methods are known as good tools to attain a PBSD owing to their ability to predict structural damage levels. These methods are generally based on logical fundamentals and effective in structural analysis and design since they can control structural displacements and consequently, evaluate damage state and collapse risk. Accordingly, new design methods based on displacements have been newly suggested. One of these approaches is the direct displacement-based design (DDBD), firstly proposed by Priestley [3]. The DDBD includes several steps, which one of which is to determine the seismic deformation of an inelastic Single-Degree-of-Freedom (SDOF) system replacing the first mode of vibration of the Multi-Degree-of-Freedom (MDOF) system. In some of the current procedures, this step is performed by approximate methods in which the nonlinear system is replaced by an equivalent linear system [4, 5].

In the direct displacement-based seismic design, determination of the lateral displacement pattern at first yielding is needed. Priestley et al. [6] suggested some relations to obtain yield displacements of eccentrically braced frames. These equations were obtained according to fundamentals of mechanics science. Furthermore, Dimopoulos et al. [7] suggested simple equations for determination lateral displacements at first yielding of moment resisting and concentrically braced steel frames.

The aim of this article is to propose a new relation for calculating the yield displacements of eccentrically braced frames. This equation is described in terms of structural properties of frames and is determined according to many case studies including nonlinear time history analyses of 30 eccentrically braced frames during 15 earthquake ground motions. The existing relations are considered for SDOF, while the proposed relation for MDOF, takes into account the distribution of yield displacement at the height of structure based on geometric properties of the structure.

*Corresponding Author Email: *hsaffari@mail.uk.ac.ir* (H. Saffari)

Please cite this article as: M. J. Zahedi, H. Saffari, Seismic Yield Displacement Profile in Steel Eccentrically Braced Frames, International Journal of Engineering (IJE), IJE TRANSACTIONS C: Aspects Vol. 32, No. 9, (September 2019) 1248-1259

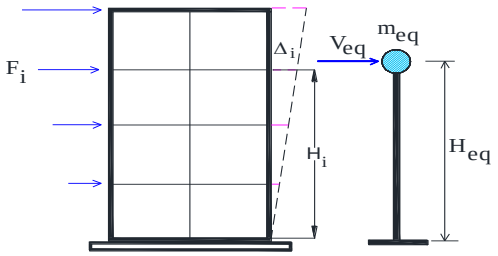

(a) SDOF representation

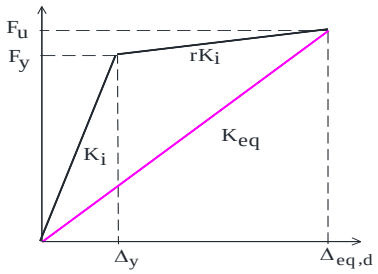

(b) Effective Stiffness, Keq

Figure 1. Equivalent SDOF Structure Characterization

2. FUNDAMENTAL OF DDBD METHOD

Figure 1(a) dipicts the basis of DDBD, in which a MDOF system replaced by a SDOF system. The DDBD describes a structure by secant stiffness K_{eq} at peak displacement, as shown in Figure 1(b). The basic steps of the DDBD method are concisely explained in the following [8]:

Step 1: Selection of the target drift according to the predefined performance.

Step 2: Selection of the displacement pattern of the frame. The design displacements Δ_i at various stories (i) can be obtained from displacement pattern.

Step 3: Computing system equivalent displacement ($\Delta_{eq,d}$): this is calculated using the displacement pattern from step 2 and the masses (m_i) at each story. It represents the equivalent system displacement of the SDOF substitute structure and is described as follows:

$$\Delta_{eq,d} = \frac{\sum_{i=1}^{n} m_i \Delta_i^2}{\sum_{i=1}^{n} m_i \Delta_i} \quad (1)$$

Step 4: Computing the effective mass and height: From consideration of mass participation in the fundamental mode, the effective system mass for the equivalent SDOF system is:

$$m_{eq} = \sum_{i=1}^{n} \left(\frac{m_i \Delta_i}{\Delta_{eq,d}} \right) \quad (2)$$

Moreover, the equivalent height (H_{eq}) should be determined as:

$$H_{eq} = \sum_{i=1}^{n} m_i \Delta_i H_i \; / \sum_{i=1}^{n} m_i \Delta_i \quad (3)$$

Step 5: Determination of design displacement ductility (μ_{eq}):

$$\mu_{eq} = \frac{\Delta_{eq,d}}{\Delta_{eq,y}} \quad (4)$$

where $\Delta_{eq,y}$ is the equivalent yield displacement determined by equations such as those proposed in the current paper.

Step 6: Choosing equivalent viscous damping: Damping is obtained as a function of displacement ductility. Such relationships are shown in Figure 2a for various kinds of structural systems. For steel frame building the following expression is introduced [6].

$$\xi_{equ} = 0.05 + 0.577 \left(\frac{\mu_{equ} - 1}{\mu_{equ} . \pi} \right) \quad (5)$$

Step 7: Determination of the system effective period: the equivalent period at peak displacement response is extracted from the displacement spectra, entering with the design displacement $\Delta_{eq,d}$ and determining the period, T_{eq} corresponding to the computed equivalent viscous damping (Figure 2b).

Step 8: Determination of design base shear: when the effective period of the substitute structure is calculated in Step 7, the effective stiffness (K_{eq}) is determined using Equation (7). The effective stiffness of the substitute structure is defined as the secant stiffness to maximum response, as drawn in Figure 1(b). The design base shear force (V_{eq}) at the specific performance level is then computed by multiplying the effective stiffness by the system displacement.

$$K_{eq} = 4\pi^2 m_{eq} / T_{eq}^2 \quad (6)$$

$$V_{eq} = K_{eq} \Delta_{eq,d} \quad (7)$$

3. DERIVATION OF THE YIELD DISPLACEMENT PATTERN

3. 1. Description of the Case Study Structures To obtain the geometrical parameters of EBFs that substantially influence the shape of the yield pattern, a group of thirty eccentrically braced frames was used. A typical configuration of 2-D frames is shown in Figure 3. The uniform story height and bay length are 144 and 360 in, respectively. The numbers of stories of the take the values of 3, 6, 9, 12 and 15. Taking the link length, *e*,

equal to *aL* (see Figure 3), six values of 0.1, 0.2, 0.3, 0.4, 0.5 and 0.6 are assigned for parameter *a*, in the design phase.

All frames have three bays with simple beam-to-column connections. The uniform dead and live loads of all beams are 0.12 and 0.06 kips/in, respectively. The EBFs have been designed based on AISC 360-10 [9], AISC 341-10 [10] and ASCE7-10 [11] using ETABS [12] software. All frames are assumed to be founded on firm soil, class C of NEHRP, and located in the region of the highest seismicity. The yield strength of steel is assumed as $F_y = 50\ ksi$ for all structural members. Final section sizes of all frames are summarized in Table 1. In this table, phrases like 3(14x311) +3(14x132) show that the first three stories possess columns with W14x311 section sizes, while the three higher stories possess columns with W14x132 section sizes.

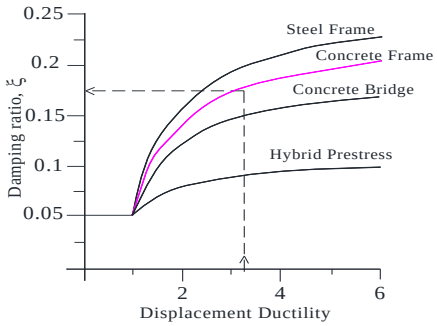

(a) Equivalent Damping vs. Ductility

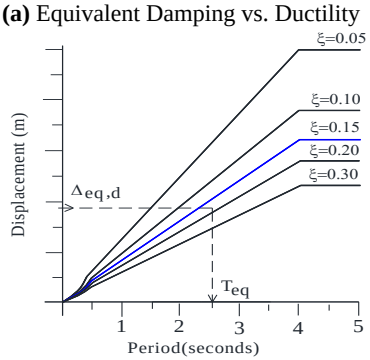

(b) Displacement Spectrum

Figure 2. Obtaining SDOF Structure Effective Period

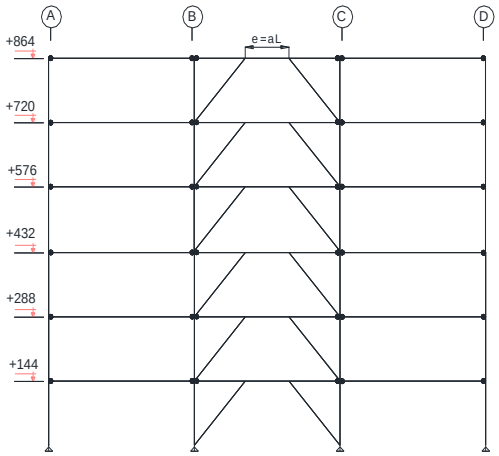

Figure 3. Six-story frame considered in the parametric studies

TABLE 1. Section sizes of models used in the parametric studies

n_s	a	Column A,D (W)	Column B,C (W)	Interior beam including link (W)	Exterior beam in all stories (W)	Brace (HSS)
3	0.1	3(14x30)	3(14x132)	3(14x48)	14x109	2(6x1/2)+6x1/4
	0.2	3(14x30)	3(14x132)	14x53+2(14x48)	14x109	6x1/2+2(6x1/4)
	0.3	3(14x30)	3(14x132)	2(14x53)+14x48	14x109	6x1/2+2(6x1/4)
	0.4	3(14x30)	3(14x132)	2(14x68)+14x53	14x109	8x1/2+6x1/2+6x1/4
	0.5	3(14x30)	3(14x176)	2(14x68)+14x53	14x109	8x1/2+6x1/2+6x1/4
	0.6	3(14x30)	3(14x176)	2(14x132)+14x82	14x109	2(6x1/2)+6x1/4
6	0.1	3(14x38)+3(14x38)	3(14x311)+3(14x132)	2(14x53)+4(14x48)	14x109	5(6x1/2)+6x1/4
	0.2	3(14x38)+3(14x30)	3(14x311)+3(14x132)	2(14x68)+4(14x48)	14x109	3(6x1/2)+3(6x1/4)
	0.3	3(14x38)+3(14x30)	3(14x311)+3(14x132)	4(14x68)+2(14x48)	14x109	3(6x1/2)+3(6x1/4)
	0.4	3(14x38)+3(14x30)	3(14x311)+3(14x132)	14x82+2(14x74)+2(14x68)+14x48	14x109	4(6x1/2)+2(6x1/4)
	0.5	3(14x38)+3(14x30)	3(14x426)+3(14x176)	2(14x132)+4(14x68)	14x109	6x1/4
	0.6	3(14x38)+3(14x30)	3(14x426)+3(14x176)	4(14x132)+2(14x68)	14x109	4(6x1/2)+2(6x1/4)
9	0.1	3(14x48)+3(14x38)+3(14x30)	3(14x500)+3(14x311)+3(132)	4(14x53)+5(14x48)	14x109	7(6x1/2)+2(6x1/4)

	0.2	3(14x48)+3(14x38)+ 3(14x30)	3(14x500)+3(14x311)+3(132)	3(14x68)+2(14x53)+4(1 4x48)	14x109	7(6x1/2)+2(6x1/4)
	0.3	3(14x48)+3(14x38)+ 3(14x30)	3(14x500)+3(14x311)+3(132)	6(14x68)+ 14x53+2(14x48)	14x109	6(6x1/2)+3(6x1/4)
	0.4	3(14x48)+3(14x38)+ 3(14x30)	3(14x500)+3(14x311)+3(132)	3(14x82)+2(14x74)+ 3 (14x68)+14x48	14x109	7(6x1/2)+2(6x1/4)
	0.5	3(14x48)+3(14x38)+ 3(14x30)	3(14x665)+ 3(14x426)+3(14x176)	5(14x132)+ 14x82+3(14x68)	14x109	6(6x1/2)+3(6x1/4)
	0.6	3(14x48)+3(14x38)+ 3(14x30)	3(14x665)+ 3(14x426)+3(14x176)	7(14x132) +2(14x68)	14x109	7(6x1/2)+2(6x1/4)
	0.1	3(14x61)+3(14x48)+3(14x 38)+3(14x30)	3(14x665)+3(14x500)+3(14x3 11)+3(14x132)	4(14x68)+2(14x53)+6(1 4x48)	14x109	9(6x1/2)+3(6x1/4)
	0.2	3(14x61)+3(14x48)+3(14x 38)+3(14x30)	3(14x665)+3(14x500)+3(14x3 11)+3(14x132)	8(14x68)+4(14x48)	14x109	9(6x1/2)+3(6x1/4)
	0.3	3(14x61)+3(14x48)+3(14x 38)+3(14x30)	3(14x665)+3(14x500)+3(14x3 11)+3(14x132)	3(14x132)+4(14x82)+3(14x74)+2(14x68)	14x109	9(6x1/2)+3(6x1/4)
12	0.4	3(14x61)+3(14x48)+3(14x 38)+3(14x30)	3(14x665)+3(14x500)+3(14x3 11)+3(14x132)	3(14x132)+4(14x82)+3(14x74)+2(14x68)	14x109	8x1/2+8(6x1/2)+3(6x1/4)
	0.5	3(14x61)+3(14x48)+3(14x 38)+3(14x30)	3(14x730)+3(14x665)+3(14x4 26)+3(14x176)	9(14x132)+ 14x82+ 14x74+ 14x68	14x109	6(8x1/2)+3(6x1/2)+ 3(6x1/4)
	0.6	3(14x61)+3(14x48)+3(14x 38)+3(14x30)	3(14x730)+3(14x665)+3(14x4 26)+3(14x176)	12(14x132)	14x109	7(8x1/2)+ 3(6x1/2)+2(6x1/4)
	0.1	3(14x68)+ 3(14x61)+3(14x48)+3(14x 38)+3(14x30)	3(14x730)+3(14x665)+3(14x5 00)+3(14x311)+ 3(14x132)	8(14x68)+ 2(14x53)+ 5(14x48)	14x109	5(8x1/2)+ 8(6x1/2)+2(6x1/4)
	0.2	3(14x68)++3(14x61)+3(14 x48)+3(14x38)+3(14x30)	3(14x730)+3(14x665)+3(14x5 00)+3(14x311)+ 3(14x132)	14x132+2(14x82)+ 3(14x74)+ 9(14x68)	14x109	5(8x1/2)+ 8(6x1/2)+2(6x1/4)
	0.3	3(14x68)+ 3(14x61)+3(14x48)+3(14x 38)+3(14x30)	3(14x730)+3(14x665)+3(14x5 00)+3(14x311)+ 3(14x132)	7(14x132)+3(14x82)+ 2(14x74)+ 2(14x68)	14x109	5(8x1/2)+ 8(6x1/2)+2(6x1/4)
15	0.4	3(14x68)++3(14x61)+3(14 x48)+3(14x38)+3(14x30)	6(14x730)+ 3(14x500)+3(14x370)+ 3(14x145)	10(14x132)+ 14x82+ 14x74+ 3(14x68)	14x109	7(8x1/2)+ 6(6x1/2)+2(6x1/4)
	0.5	3(14x68)++3(14x61)+3(14 x48)+3(14x38)+3(14x30)	6(14x730)+ 3(14x665)+3(14x426)+ 3(14x176)	2(14x159)+ 3(14x145)+ 7(14x132)+ 14x82+ 14x74+ 14x68	14x109	9(8x1/2)+ 5(6x1/2)+ 6x1/4
	0.6	3(14x68)++3(14x61)+3(14 x48)+3(14x38)+3(14x30)	6(14x730)+ 3(14x665)+3(14x426)+ 3(14x176)	5(14x176)+ 2(14x159)+ 2(14x145)+ 5(14x132)+ 14x68	14x109	11(8x1/2)+ 3(6x1/2)+ 6x1/4

3. 2. Seismic Excitation Fifteen different ground motions are considered for the nonlinear time history analysis of this study. This category includes both far field and near field records [13-15]. The near field ground motions have been selected from SAC [16] database, whereas far field records have been selected from FEMA P695 [17]. The records are available in the Pacific Earthquake Engineering Research (PEER) site,http://peer.berkeley.edu/smcat. The basic parameters of the records are summarized in Table 2. In addition, their elastic response spectra are shown in Figure 4.

3. 3. Framework of the Present Study All 30 EBFs of Table 1 are analyzed to obtain their behavior under each one of the 15 ground motions mentioned in Table 2. The OPENSEES [18] software is used for the nonlinear time history analyses. In EBFs, the inelastic behavior of the link beam is simulated by using an approach presented by Bosco et al. [19]. The model considers the influence of the shear force and bending moment on the inelastic behavior of the link beams with short intermediate and long lengths.

The link model involves five elements connected in series, as drawn in Figure 5. The mid element (EL0) has the same length and moment of inertia of the link and considers the flexural elastic behavior of the link. In spite of (EL1) that considers the elastic and inelastic shear behavior of half a link, (EL2) considers the inelastic

TABLE 2. Characteristics of earthquake ground motions

RSN*	Component	Magnitude	Rjb(km)**	Arias Intensity (m/s)
821	EW	6.69	0	1.789
1106	000	6.9	0.94	8.393
1120	000	6.9	1.46	8.697
879	260	7.28	2.19	6.972
3548	000	6.93	3.22	1.863
828	000	7.01	0	3.414
1063	228	6.69	0	7.513
143	L1	7.35	1.79	11.822
125	000	6.5	14.97	0.786
169	262	6.53	22.03	2.389
1116	000	6.9	19.14	0.826
848	000	7.28	19.74	3.141
900	270	7.28	23.62	0.923
752	000	6.93	15.23	4.406
953	009	6.69	9.44	3.087

*RSN: Record Sequence Number in PEER

**Rjb: The closest horizontal distance to the surface projection of the rupture plane (Joyner-Boore distance to Rupture plane)

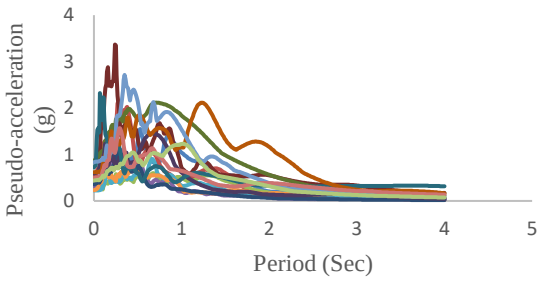

Figure 4. Acceleration spectra of the 15 selected ground motions

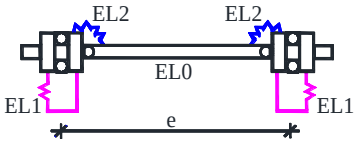

Figure 5. Simulation of the link [19]

flexural behavior of the ending part of the link. The nodes of EL1 and EL2 are allowed to have independently relative vertical displacements and relative rotations, orderly [19]. In OpenSees modeling, for springs EL1 and EL2 BrbDallAsta material used and for other members elasticBeamColumn element has been used.

For every pair of structure and ground motion, the scale factors (SF) of the ground motion which corresponding to the occurrence of the first plastic hinge [20, 21] were determined by Incremental Dynamic Analysis (IDA). The response based on floor displacements at the first yielding time in plastic hinges was recorded to create the databank for EBFs.

The responses of the nonlinear time history analyses (30 EBF * 15 accelerograms =450 nonlinear dynamic analyses) are post-processed for statistical analyses and for obtaining the yield displacement pattern.

4. RESULTS OF PARAMETRIC STUDIES AND SUGG ESTED RELATIONS

4. 1. Computational Results For every structure, 15 yield displacement patterns are acquired. The median value of the peak displacement of the jth story, $U_{m,j}$, defined as the geometric mean, of n accelerograms, and the dispersion measures, $\sigma_{m,j}$, defined as the standard deviation of logarithm of the n accelerograms are computed by the following relations [22]:

$$U_{m,j} = \exp\left(\frac{\sum_{i=1}^{n} \mathrm{Ln}U_{i,j}}{n}\right) \quad (8)$$

$$\sigma_{m,j} = \sqrt{\frac{\sum_{i=1}^{n}\left(\mathrm{Ln}U_{i,j} - \mathrm{Ln}U_{m,j}\right)^2}{n-1}} \quad (9)$$

where $U_{i,j}$ is the peak displacement of the jth story under the ith ground motion.

Figures 6 to 15 show the median yield displacement and dispersion values for frames with different link length ratios. The following conclusions can be drawn from the results of the present study:

For the frames having the same stories but different link length ratio, the yield patterns are almost identical at the short link, some different at the moderate link and considerably different at the long link. With the increase of link length ratio, the inter-story deformation distributes non-uniformly along the height Dispersion is small at the short link and with the increase of link length the larger value of dispersion appears at the middle stories.

4. 2. Suggested Relations The databank for the EBFs was obtained as a function of the frame features like $\frac{h_i}{H}$, $\frac{e}{L_{bay}}$ and n_s where h_i is the story's height, H is the total frame height, e is the link length, L_{bay} is the bay length and n_s is numbers of stories. The Levenberg-Marquardt algorithm of SPSS software [23] is used for

nonlinear regression analysis of the mean from 270 values of floor yield displacements of every frame for the seismic motions.

After processing the obtained databank for the EBFs, the influences of the different parameters of the structures on yield displacements were specified and the following relation is proposed,

$$\Delta_{y,i} = \varepsilon_y n_s^{-0.50} h_i^{1.412} \left(\frac{h_i}{H}\right)^{-0.55} \left(\frac{e}{L_{bay}}\right)^{1.6} \quad (10)$$

where i represents the i[th] floor and ε_y is yield strain of steel.

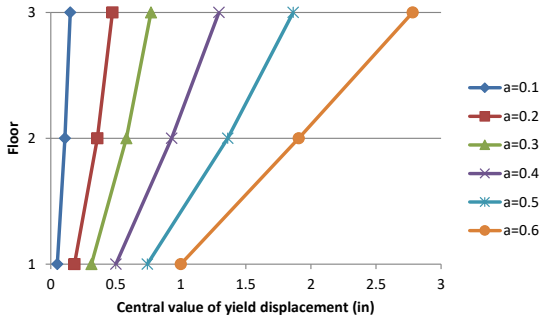

Figure 6. Central values of yield displacements for 3-story frame

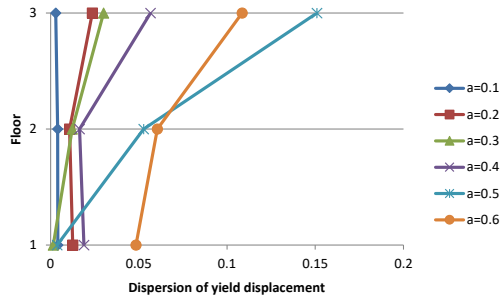

Figure 7. Dispersion of yield displacements for 3-story frame

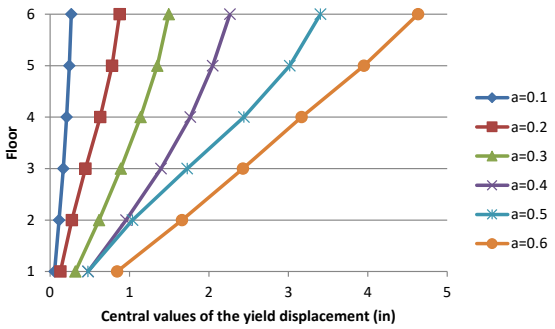

Figure 8. Central values of yield displacements for 6-story frame

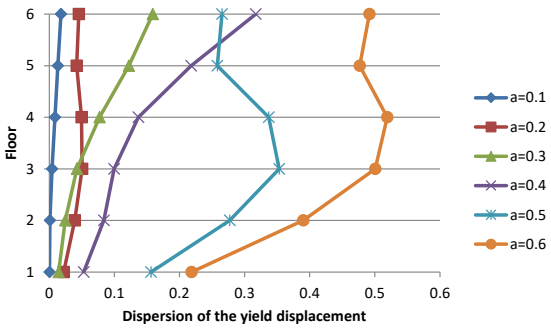

Figure 9. Dispersion of yield displacements for 6-story frame

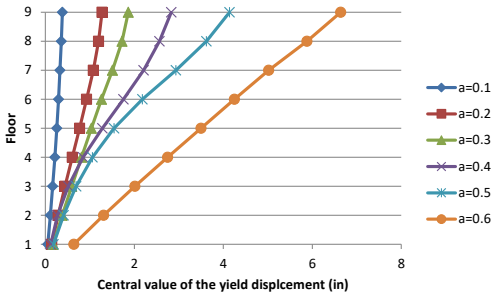

Figure 10. Central values of yield displacements for 9-story frame

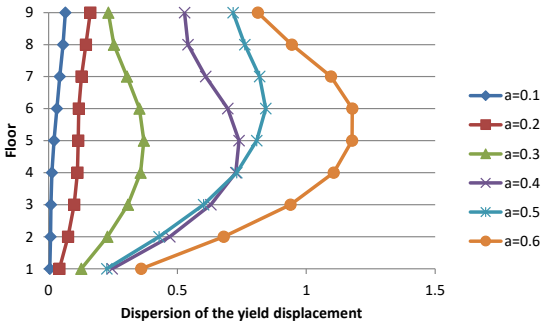

Figure 11. Dispersion of yield displacements for 9-story frame

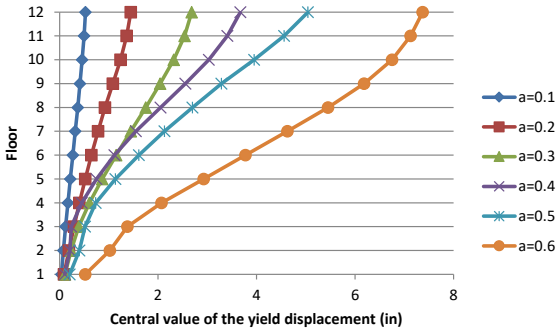

Figure 12. Central values of yield displacements for 12-story frame

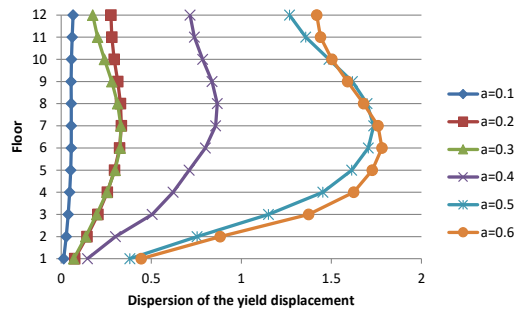

Figure 13. Dispersion of yield displacements for 12-story frame

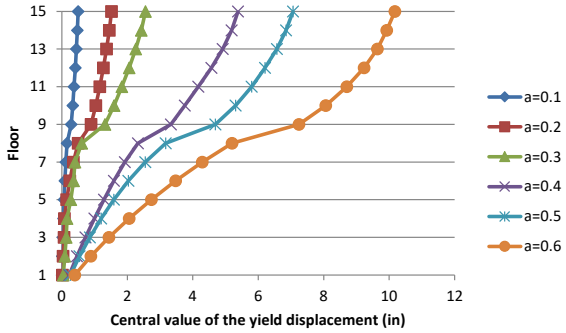

Figure 14. Central values of yield displacements for 15-story frame

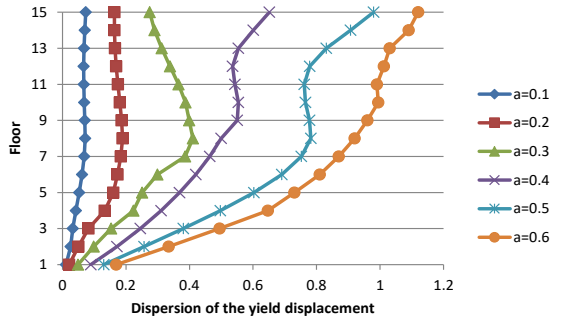

Figure 15. Dispersion of yield displacements for 15-story frame

5 .COMPARISON OF YIELD DISPLACEMENT RELATIONS IN EBFS

In the following, the suggested expression is compared with some existing methods.

5. 1. Tested Structures The three 6-story EBFs with different link to span length ratios used as tested frames have been designed according to AISC 360-10 [9], AISC 341-10 [10] and ASCE7-10 [11] using ETABS [12] software. The uniform story height and bay length are 120 and 300 in, respectively. Additionally, the uniform dead and live loads of all beams are 0.12 and 0.06 kips/in, respectively. Final section sizes of these frames are summarized in Table 3.

5. 2. Priestley et al. [6] Relations Priestley et al. [6] recommend relations for the yield displacement in EBFs as follows:

- The story yield drift ratio for the flexural link:

$$\theta_{y,f} = \varepsilon_y \frac{L_{bay}}{H_s} + C_1 \frac{Z_p \varepsilon_y l_1^2}{6I.L_{bay}} \quad (11)$$

where ε_y is yield strain of steel, L_{bay} is bay length, H_s is story height, Z_p is plastic modulus of beam section, l_1 is link length, I is moment of inertia of beam section, C_1 is defined as:

$$C_1 \approx\sim 1+2\frac{h_1}{L_{bay}} \quad (12)$$

where h_1 is web depth of beam section.

- The story yield drift ratio for shear link:

$$\theta_{y,s} = \varepsilon_y \frac{L_{bay}}{H_s} + \frac{0.55 h_1 t_{wb} \varepsilon_y l_1^3}{12I.L_{bay}} \quad (13)$$

t_{wb} is web thickness of link beam.

The story yield drift ratio for intermediate link should be determined by linear interpolation between Equations (11) and (13).

TABLE 3. The geometric characteristics of tested EBFs

ns	a	Column A,D (W)	Column B,C (W)	Interior beam including link (W)	Exterior beam (W)	brace (HSS)
6	0.1	14x38(1-3)+ 14x26(4-6)	14x283(1-3)+ 14x132(4-6)	14x48(all)	14x53(1-6)	6x1/2(1-3)+ 6x1/4(4-6)
	0.3	14x38(1-3)+ 14x26(4-6)	14x426(1-3)+ 14x132(4-6)	14x68(1-4)+ 14x48(5-6)	14x53(1-6)	6x1/2(1)+ 6x1/4(2-6)
	0.6	14x38(1-3)+ 14x30(4-6)	14x605(1-3)+ 14x257(4-6)	14x82(1-3)+ 14x74(4 14x68(5-6)	14x53(1-6)	6x1/2(1-4)+ 6x1/4(5-6)

It is usually enough precise to suppose a linear yield displacement pattern for the goal of approximating ductility demand, and thus the yield displacement is obtained by:

$$\Delta_y = \theta_y H_{eq} \tag{14}$$

where H_{eq} is previously defined.

5. 3. Comparison of Yield Displacements The yield displacement patterns of three EBFs are depicted in Figures 16–18. As can be seen, the suggested pattern has good agreement with nonlinear dynamic analyses in all studied frames. Besides, one of the advantages of the suggested method is the approximation of yield displacement at height easily in comparison with other methods.

Moreover, the SDOF displacements at first yielding are computed using the suggested expression, Priestley r elations [6] and nonlinear dynamic analyses (Figures 19 –21). As can be noticed, the SDOF yield displacement o f the suggested relation is consistent with that of nonline ar dynamic analyses and delivers more accurate predictions than others.

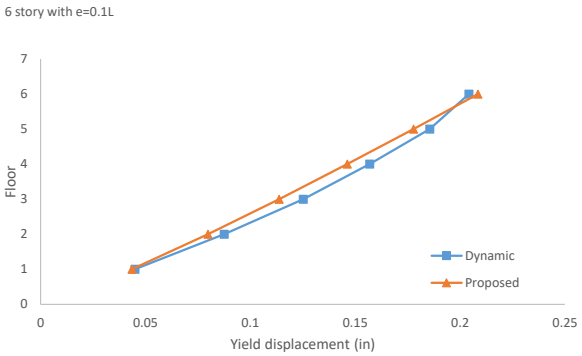

Figure 16. Comparison of yield displacements patterns for 6-story frame with e=0.1L

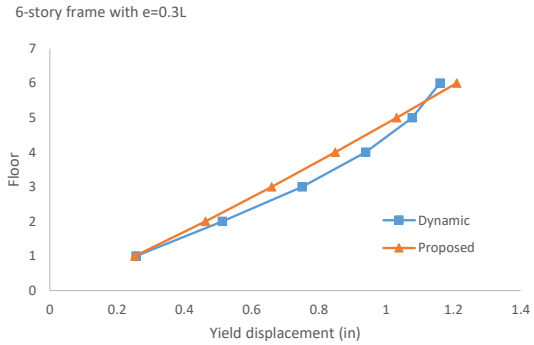

Figure 17. Comparison of yield displacements patterns for 6-story frame with e=0.3L

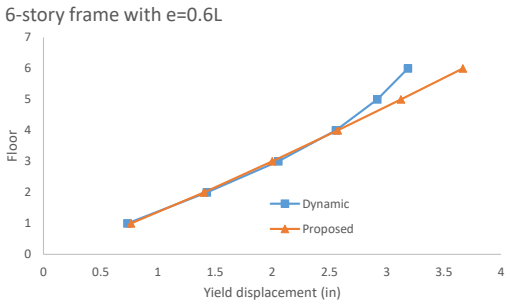

Figure 18. Comparison of yield displacements patterns for 6-story frame with e=0.6L

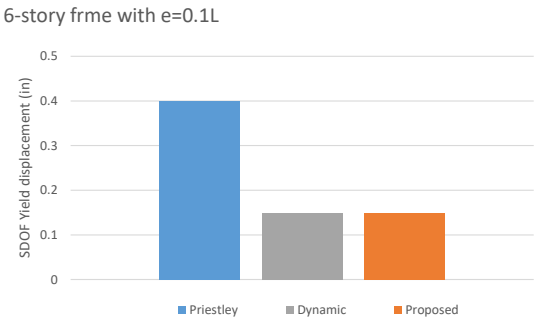

Figure 19. SDOF yield displacements, obtained from different methods for 6- story frame with e=0.1L

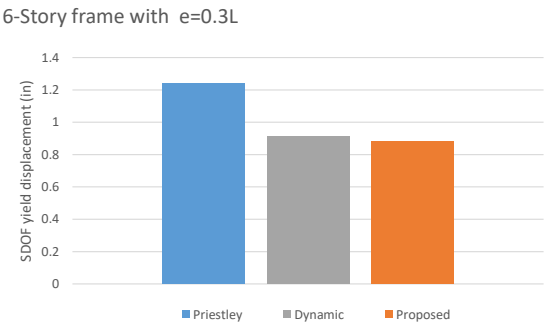

Figure 20. SDOF yield displacements, obtained from different methods for 6- story frame with e=0.3L

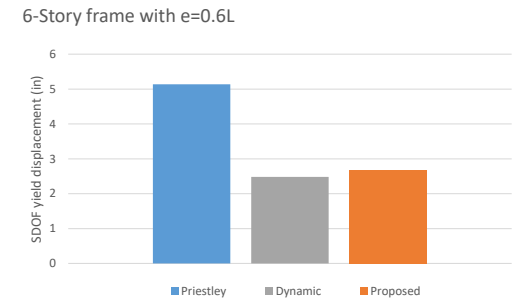

Figure 21. SDOF yield displacements, obtained from different methods for 6- story frame with e=0.6L

The existing relations are considered for SDOF, while the proposed relation for MDOF, takes into account the distribution of yield displacement at the height of structure based on geometric properties of the structure. This feature makes good agreement with dynamic analysis result. In other hand, the computational effort of method is more than existing method.

5. 4. Obtaining of Displacement Patterns Based on N2 Method In this study for predicting maximum floor displacements of EBFs, the N2 method [24] as the usual nonlinear procedure is employed. In this technique, inelastic demand spectra are obtained from the elastic design spectra and are converted into acceleration displacement response spectra (ADRS) format. This is the demand spectrum and the intersection of the capacity spectrum and demand spectrum estimates the inelastic acceleration and displacement demand. Capacity diagrams are idealized with elastic-perfectly plastic curves [25].

The load pattern that was used in this study is the first mode pattern, namely, where is the lumped mass at ith is the first mode shape at ith floor. For example the performance point for 6-story frame with e=0.6L based on ASCE 7-10 [11] spectrum for soil class C and is shown in Figure 22. Furthermore, the target displacement patterns according to N2-method and SDOF design displacements Δeq,d are shown in Table 4.

5. 5. Comparison of Base Shears in DDBD Method To compare the base shears outcomes of the suggested expression with those of other available expressions, nonlinear time history analyses are done employing seven ground motions from the PEER site (http: //peer.berkeley.edu/smcat). Such seven ground motions were scaled by SeismoMatch software in order to determine an average pseudo-acceleration spectrum matching the elastic spectrum supposed for the design, in accordance with ASCE 7-10 [11]. Spectra of the selected ground motions are shown in Figure 23 together with the average spectrum and the elastic spectrum.

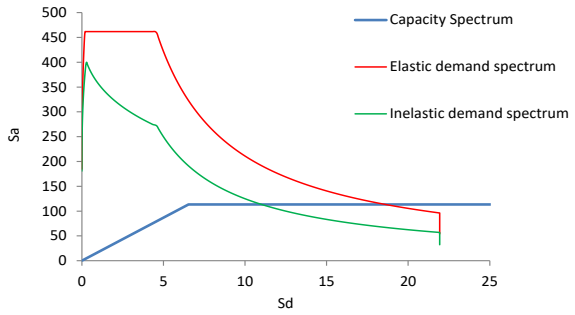

Figure 22. Obtaining performance point according to N2-m ethod [22] for 6-story frame with e=0.6L based on ASCE 7-10 spectrum

TABLE 4. Target displacement patterns based on N2-method and SDOF design displacements $\Delta_{eq,d}$

Frame	Δ_1	Δ_2	Δ_3	Δ_4	Δ_5	Δ_6	$\Delta_{eq,d}$
6-story with e=0.1L	2.44	4.58	6.21	7.15	7.67	8.00	4.66
6-story with e=0.3L	2.45	4.74	6.73	8.11	8.97	9.52	7.67
6-story with e=0.6L	3.31	6.49	9.42	11.81	13.43	14.59	11.42

Figure 24 shows the pseudo-acceleration and displacement spectra with various damping values as determined from the corresponding design spectrum of ASCE 7-10 [11] for soil class C and $S_s = 1.7865, S_1 = 0.8589$ .The damping modifier R_ζ should be applied to the elastic displacement spectrum for various levels of damping ζ according to Newmark and Hall relation [26] as following:

$$R_\zeta = 1.31 - 0.19Ln(100\zeta) \quad (15)$$

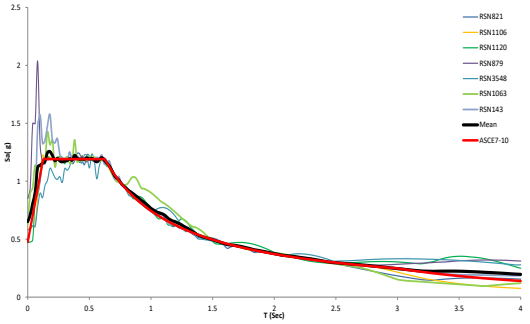

Figure 23. Seven elastic design spectrum accelerograms compatible to ASCE-7 spectrum

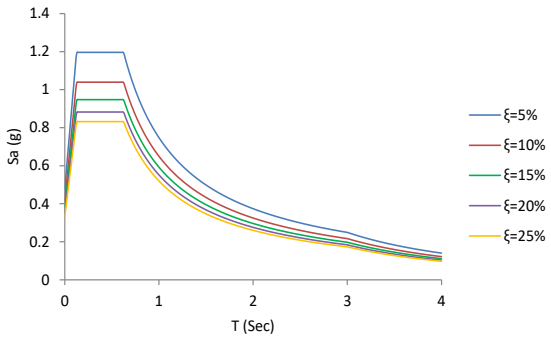

(a) Pseudo-acceleration response spectrum

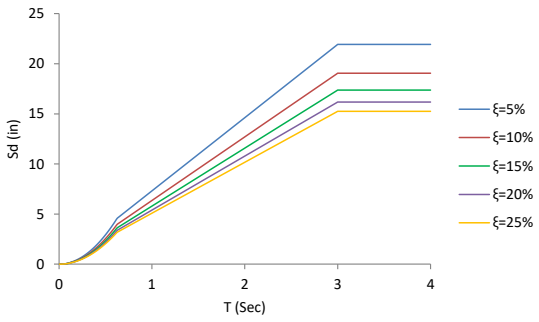

(b) displacement response spectrum

Figure 24. ASCE-7 design spectrum used for the DDBD process

Based on the DDBD method as described in section 2, the parameters of substitute structure for 3 tested frames are listed in Table 5.

The base shears are calculated and compared to those determined by the DDBD method in Table 6. As observed in table, suggested relation has good agreement with the dynamic analyses in compared to those of the Priestley et al. [6] method in all studied frames. The suggested relation is more precise particularly in flexural links in comparison with other methods.

6. SUMMARY AND CONCLUSIONS

In the direct displacement-based seismic design method, the seismic yield displacement is applied as the design parameter. A new equation for the determination of lateral yield displacements of EBF subjected to earthquake ground motions has been suggested to be employed in the DDBD method or other approaches which need information about this type of displacements. This expression has been determined within a statistical analysis of the outcomes of hundreds of nonlinear dynamic analyses. The dispersion of the peak yield displacement was calculated by the coefficient of variance. Results show that the suggested relation has good agreement with nonlinear dynamic analyses.

Moreover, comparison of the suggested relation versus other present expressions indicates the precision of the suggested one.

TABLE 5. DDBD parameters calculated for Equivalent SDOF frames

Frame	Method	$\Delta_y\,(in)$	μ_{eq}	$\xi_{eq}\,(\%)$	$T_{eq}\,(s)$	$K_{eq}\,(kips/in)$	$V_{eq}\,(kips)$
6-story frame with e=0.1L	Priestley et al. [6]	0.4	11.66	21.79	0.88	135.24	631.25
	Suggested Equation (12)	0.15	31.1	22.77	0.89	132.23	617.03
6-story frame with e=0.3L	Priestley et al. [6]	1.24	6.18	20.4	1.43	47.95	367.81
	Suggested Equation (12)	0.88	8.71	21.26	1.44	46.96	360.21
6-story frame with e=0.6L	Priestley et al. [6]	5.14	2.22	15.10	1.80	29.44	336.41
	Suggested Equation (12)	2.68	4.26	19.05	2.09	21.85	249.72

TABLE 6. Comparison of base shears from dynamic analyses and DDBD methods

	Frame	Base shears of 6-story with e=0.1L	Base shears of 6-story with e=0.3L	Base shears of 6-story with e=0.6L
DDBD	Priestley et al. [6]	631.25	367.81	336.41
	Suggested Equation (12)	617.03	360.21	249.72
Nonlinear dynamic analyses	RSN821_ERZINCAN_ERZ-EW	577.38	361.60	234.78
	RSN1106_KOBE_KJM000	465.81	362.78	218.88
	RSN1120_KOBE_TAK000	451.29	325.05	195.72
	RSN879_LANDERS_LCN260	481.71	242.60	199.81
	RSN3548_LOMAP_LEX000	573.24	384.44	260.33
	RSN1063_NORTHR_RRS228	416.98	281.47	203.92
	RSN143_TABAS_TAB-L1	546.70	375.26	226.00
	AVE	501.87	333.32	219.92
Errors (%)	Priestley et al. [6]	25.73	10.34	52.96
	Suggested Equation (12)	22.94	8.00	13.55

7. REFERENCES

1. Rubinstein, M., Moller, O. and Giuliano, A., "Inelastic displacement-based design approach of r/c building structures in seismic regions", ***Structural Engineering and Mechanics***, Vol. 12, No. 6, (2001), 573-594.
2. Vafaee, M.H. and Saffari, H., "A modal shear-based pushover procedure for estimating the seismic demands of tall building structures", ***Soil Dynamics and Earthquake Engineering***, Vol. 92, No., (2017), 95-108.
3. Priestley, M.N., "Myths and fallacies in earthquake engineering-conflicts between design and reality", Bulletin of the New Zealand National Society for Earthquake Engineering, Vol. 26, No. 3, (1993), 329-341.
4. Gulkan, P. and Sozen, M.A., "Inelastic responses of reinforced concrete structure to earthquake motions", in Journal Proceedings. Vol. 71, (1974), 604-610.
5. Gulkan, P. and Sozen, M., "Substitute structure method for seismic design in reinforced concrete", ***A***CI Journal, Dec, (1974).
6. Calvi, G., Priestley, M. and Kowalsky, M., "Displacement based seismic design of structures", in New Zealand Conference on Earthquake Engineering, 2007, Citeseer. (2007).
7. Dimopoulos, A.I., Bazeos, N. and Beskos, D.E., "Seismic yield displacements of plane moment resisting and x-braced steel frames", ***Soil Dynamics and Earthquake Engineering***, Vol. 41, No., (2012), 128-140.
8. Amiri, G.G., Shalmaee, M.M. and Namiranian, P., "Evaluation of a ddb design method for bridges isolated with triple pendulum bearings", ***Structural Engineering and Mechanics***, Vol. 59, No. 5, (2016), 803-820.
9. ANSI, A., "Aisc 360-10", Chicago, IL, (2010).
10. AISC, A., "Aisc 341-10, seismic provisions for structural steel buildings", Chicago, IL: American Institute of Steel Construction, (2010).
11. Engineers, A., "Minimum design loads for buildings and other structures", ASCE 7, Vol. 10, (2010).
12. Habibulah, A., *Etabs (extended three dimensional analysis of building systems)*. 1995, User's Manual, Computers and Structures Inc., Berkeley, California.
13. Eskandari, R. and Vafaei, D., "Effects of near-fault records characteristics on seismic performance of eccentrically braced frames", ***Structural Engineering and Mechanics***, Vol. 56, No. 5, (2015), 855-870.
14. Kamgar, R. and Rahgozar, R., "Determination of critical excitation in seismic analysis of structures", ***Earthquakes and Structures***, Vol. 9, No. 4, (2015), 875-891.
15. Kamgar, R., Samea, P. and Khatibinia, M., "Optimizing parameters of tuned mass damper subjected to critical earthquake", ***The Structural Design of Tall and Special Buildings***, Vol. 27, No. 7, (2018), e1460.
16. Venture, S.J., "Develop suites of time histories, project task: 5.4. 1, draft report", Sacramento, CA, USA, March, Vol. 21, (1997).
17. ATC, F., *P695, quantification of building seismic performance factors*. 2009, Applied Technology Council, Redwood City, CA.
18. McKenna, F., Fenves, G., Filippou, F. and Scott, M., Open system for earthquake engineering simulation (opensees). Berkeley: Pacific earthquake engineering research center, university of california; *2005*. 2016.
19. Bosco, M., Marino, E.M. and Rossi, P.P., "Modelling of steel link beams of short, intermediate or long length", ***Engineering structures***, Vol. 84, No., (2015), 406-418.
20. Pekelnicky, R., Engineers, S.D., Chris Poland, S. and Engineers, N.D., "Asce 41-13: Seismic evaluation and retrofit rehabilitation of existing buildings", ***Proceedings of the SEAOC***, Vol., No., (2012).
21. Saffari, H., Damroodi, M. and Fakhraddini, A., "Assesment of seismic performance of eccentrically braced frame with vertical members", ***Asian Journal of Civil Engineering***, Vol. 2, No. 18, (2017), 255-269.
22. Cornell, C.A., Jalayer, F., Hamburger, R.O. and Foutch, D.A., "Probabilistic basis for 2000 sac federal emergency management agency steel moment frame guidelines", ***Journal of Structural Engineering***, Vol. 128, No. 4, (2002), 526-533.
23. Corp, I., "Ibm spss statistics for windows, version 22.0", Armonk, NY: IBM Corp, (2013).
24. Fajfar, P. and Gašperšič, P., "The N2 method for the seismic damage analysis of rc buildings", ***Earthquake Engineering & Structural Dynamics***, Vol. 25, No. 1, (1996), 31-46.
25. Landi, L., Pollioa, B. and Diotallevi, P.P., "Effectiveness of different standard and advanced pushover procedures for regular and irregular rc frames", ***Structural Engineering and Mechanics***, Vol. 51, No. 3, (2014), 433-446.
26. Newmark, N.M., "Earthquake spectra and design", Earthquake Eng. Research Institute, Berkeley, CA, (1982).

Seismic Yield Displacement Profile in Steel Eccentrically Braced Frames

M. J. Zahedi, H. Saffari

Department of Civil Engineering, Shahid Bahonar University of Kerman, Kerman, Iran

P A P E R I N F O

Paper history:
Received 09 January 2019
Received in revised form 24 June 2019
Accepted 05 July 2019

Keywords:
Seismic Yeild Displacement
Direct Displacement based Design
Performance Based Seismic Design
Eccentrically Braced Frames
Steel Building

چکیده

روش‌های طراحی براساس جابجایی روشی مناسب برای رسیدن به اهداف روش طراحی لرزه‌ای براساس عملکرد شناخته می‌شوند. در روش طراحی لرزه‌ای براساس جابجایی مستقیم، جابجایی تسلیم لرزه‌ای به عنوان یکی از پارامترهای مهم طراحی مورد استفاده قرار می‌گیرد. در این مقاله یک رابطه جدید برای تعیین الگوی جابجایی جانبی در اولین تسلیم سیستم قاب بادبندی واگرا تحت تحریک زمین لرزه پیشنهاد شده است. این رابطه تاثیر ویژگی مختلف سازه‌ای قاب‌ها را در نظر می‌گیرد و از نتایج چندین تحلیل دینامیکی غیرخطی که شامل ۳۰ قاب بادبندی واگرا و ۱۵ زلزله دور از گسل و نزدیک گسل می‌باشند استخراج گردیده است. سپس نتایج این آنالیزها با تحلبل رگرسیون غیرخطی جهت بدست آوردن موثرترین پارامترهای الگوی جابجایی تسلیم قاب‌ها مورد پردازش قرار گرفته‌اند. به عنوان نتیجه‌گیری، یک مقایسه بین الگوی جابجایی تسلیم پیشنهادی و نتایج حاصل از آنالیز دینامیکی غیرخطی صورت گرفت که کارایی و مزایای روش پیشنهادی را نشان می‌دهد.

***doi**: 10.5829/ije.2019.32.09c.04*